

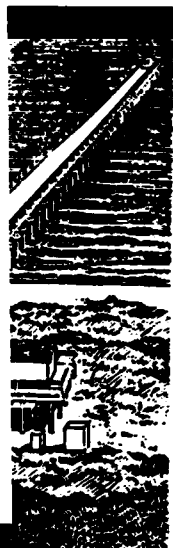
2

TECHNICAL REPORT CERC-84-7



US Army Corps
of Engineers

AD-A157 975



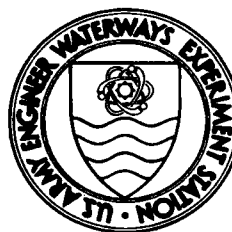
THE TMA SHALLOW-WATER SPECTRUM DESCRIPTION AND APPLICATIONS

by

Steven A. Hughes

Coastal Engineering Research Center

DEPARTMENT OF THE ARMY
Waterways Experiment Station, Corps of Engineers
PO Box 631, Vicksburg, Mississippi 39180-0631

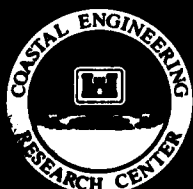
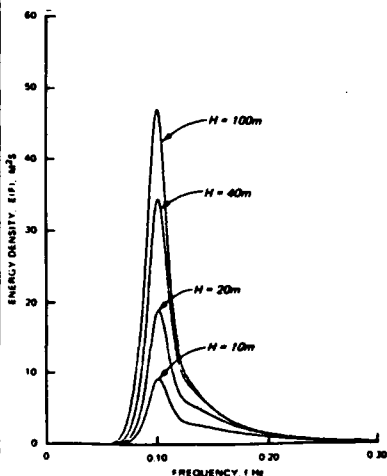


December 1984

Final Report

Approved For Public Release; Distribution Unlimited

DTIC FILE COPY



DTIC
ELECTE
AUG 13 1985
S D

Prepared for DEPARTMENT OF THE ARMY
US Army Corps of Engineers
Washington, DC 20314-1000

Under Civil Works Research Work Unit 31592

85 8 6 060

Destroy this report when no longer needed. Do not return
it to the originator.

The findings in this report are not to be construed as an official
Department of the Army position unless so designated
by other authorized documents.

The contents of this report are not to be used for
advertising, publication, or promotional purposes.
Citation of trade names does not constitute an
official endorsement or approval of the use of
such commercial products.

Accession For	
NTIS GRA&I	<input checked="checked" type="checkbox"/>
DTIC TAB	<input type="checkbox"/>
Unannounced	<input type="checkbox"/>
Justification	
By	
Distribution/	
Availability Codes	
Dist	Avail and/or Special
A-1	



SECURITY CLASSIFICATION OF THIS PAGE (When Data Entered)

DD FORM 1 JAN 73 1473 EDITION OF 1 NOV 65 IS OBSOLETE

SECURITY CLASSIFICATION OF THIS PAGE (When Data Entered)

Unclassified

SECURITY CLASSIFICATION OF THIS PAGE(When Data Entered)

20. ABSTRACT (Continued).

describe single-peaked wind seas which have reached a growth equilibrium in finite depth water. The purposes of this report are to summarize the recent advances, to discuss the range of practical usage, and to provide engineering examples using these new formulations;

Unclassified

SECURITY CLASSIFICATION OF THIS PAGE(When Data Entered)

PREFACE

The developments described in this paper are primarily a result of research conducted by an international group comprised of E. Bouws, Royal Netherlands Meteorological Institute; H. Gunther and W. Rosenthal, University of Hamburg and Max-Plank-Institut fur Meteorologie; and C. L. Vincent, Coastal Engineering Research Center (CERC), US Army Engineer Waterways Experiment Station (WES). Extensions of this basic work by C. L. Vincent and S. A. Hughes are also included.

The research summarized in this report was authorized by the Office, Chief of Engineers (OCE), US Army Corps of Engineers, under Civil Works Research Work Unit 31592, "Wave Estimation for Design." Funds were provided through the Coastal Engineering Research Area under the field management of CERC and Mr. J. H. Lockhart, Jr., OCE Technical Monitor.

This report was written by Dr. Steven A. Hughes, Research Hydraulic Engineer, under direct supervision of Dr. E. F. Thompson, Chief, Coastal Oceanography Branch and under general supervision of Drs. J. R. Houston, Chief, Research Division and R. W. Whalin, Chief, CERC.

Commander and Director of WES during the publication of this report was COL Robert C. Lee, CE. Technical Director was Mr. F. R. Brown.

CONTENTS

	<u>Page</u>
PREFACE	1
PART I: INTRODUCTION	3
PART II: SHALLOW-WATER DEVELOPMENTS	6
Equilibrium Range	6
Depth-Limited Significant Wave Height	8
TMA Spectrum	9
Wave Growth Limitation	15
PART III: SURF ZONE SPECTRA	19
Fit of TMA to Collected Spectra	19
Hypothesis for Energy Saturation	20
PART IV: DISCUSSION	27
Physical Implications of the TMA Spectral Form	27
Assumptions and Limitations of the TMA Spectral Form	28
PART V: ENGINEERING APPLICATIONS	30
Numerical Models	30
Design Example 1	30
Design Example 2	32
Design Example 3	34
Design Example 4	35
PART VI: SUMMARY	37
REFERENCES	38
APPENDIX A: NOTATION	A1

THE TMA SHALLOW-WATER SPECTRUM
DESCRIPTION AND APPLICATIONS

PART I: INTRODUCTION

1. Determination of realistic estimates for wave conditions in shallow water has always been important in coastal engineering. Initially monochromatic wave theory was used exclusively, but it is now generally accepted that an irregular wave approach is preferred. The purposes of this report are to summarize recent advances in the specification of a shallow-water self-similar spectral form, to discuss the range of practical usage, and to provide engineering examples using the new formulations.

2. The first quantitative predictions of ocean waves evolved from observations of waves at a point in space and correlations between such parameters as mean wave height, significant wave height, and mean wave period. In the mid-1950's the spectral description of the sea state was forwarded. This description allowed for more detail by distinguishing between the different frequency bands. Phillips (1958) suggested that there should be a region of the spectrum of wind-generated deepwater gravity waves in which the wave energy density has an upper bound given by the following expression:

$$E_m(f) = \alpha g^2 f^{-5} (2\pi)^{-4} \quad (1)$$

where f is frequency,* g is gravitational acceleration, and α was assumed to be a universal constant, approximately 8×10^{-3} . This region of the spectrum is called the equilibrium range. In scalar wave number space this equilibrium range becomes

$$F(k) = \beta k^{-3} \quad (2)$$

where β is a constant and k is the wave number equal to $2\pi/L$ when L is the wave length. The limit, defined by Equation 1 or 2, was thought to be a

* For convenience, symbols and abbreviations are listed in the Notation (Appendix A).

result of a limiting wave steepness at each frequency beyond which deepwater wave breaking would occur. In other words, any additional energy input in the spectrum at that frequency would result in waves breaking and a transfer of wave energy from that frequency through the mechanisms of dissipation and wave-wave interactions. This represents the equilibrium or steady-state wind sea situation in deep water, and Equation 1 describes the portion of the spectrum to the high frequency side of the single spectral peak.

3. A spectral shape for fully developed deepwater waves was advanced by Pierson and Moskowitz (1964) containing Phillips' equilibrium range (Equation 1). It is expressed as

$$E_{pm}(f) = E_m(f)e^{-5/4(f/f_m)^{-4}} \quad (3)$$

where f_m is the frequency of the spectral peak. The additional exponential term provides the low frequency forward face of the spectrum and a broad, smooth peak region. Equation 3 is based on extensive field data. Estimation of f_m for fully developed seas (i.e., no further wave growth could occur at that windspeed) was empirically determined in terms of 10-m-high windspeed U as

$$f_m = \frac{0.82g}{2\pi U} \quad (4)$$

Integration of Equation 3 provides the total energy E in the spectrum. Longuet-Higgins (1952) has shown that 4 times the variance, or $4(E)^{1/2}$, provides a close estimate of significant wave height in deep water. Thus a method exists for hindcasting and forecasting fully developed deepwater wave heights and periods.

4. One drawback to the fully developed representation was that at higher windspeeds the wind seldom held steady for the length of time necessary for fully saturated seas to develop. In other cases the fetch over which the wind acted wasn't long enough for fully developed conditions.

5. The data from the Joint North Sea Wave Program (JONSWAP) were used by Hasselmann, et al. (1973) to extend the Pierson-Moskowitz spectral density representation (Equation 3) to partially developed wave conditions by the addition of another factor:

$$E_J(f) = E_m(f) e^{-5/4(f/f_m)^{-4}} \underbrace{\gamma \exp [-(f/f_m - 1)^2 / 2\sigma^2]}_{\text{new factor}} \quad (5)$$

where

$$\alpha = 0.076 \left(\frac{gX}{U^2} \right)^{-0.22} \quad (6)$$

$$f_m = 3.5 \left(\frac{g}{U} \right) \left(\frac{gX}{U^2} \right)^{-0.33} \quad (7)$$

$$\gamma = 7.0 \left(\frac{gX}{U^2} \right)^{-0.143} \quad (\text{Mitsuyasu 1981}) \quad (8)$$

U = windspeed

X = fetch distance

$$\sigma = \begin{cases} \sigma_a = 0.07 & \text{for } f_m \geq f \\ \sigma_b = 0.09 & \text{for } f_m < f \end{cases}$$

6. The effect of the new factor is to allow for narrower, more peaked spectra which are typical of growing wind seas in deep water. Correlations were used to arrive at the parametric relationships given by Equations 6-8. Other self-similar spectral representations have been proposed for deep water (Toba 1973 and Kruseman 1976), but the JONSWAP form is the most widely known.

PART II: SHALLOW-WATER DEVELOPMENTS

Equilibrium Range

7. Kitaigorodskii et al. (1975) examined the possibility that an equilibrium range existed also for the finite depth horizontal bottom case. They noted that while both forms of the equilibrium range given for deep water (Equations 1 and 2) are valid, only one of them could hold simultaneously for deep and shallow water. Since wave breaking occurs in both deep and shallow water, it is reasonable to believe that the similarity form must be consistent between deep and shallow water. Field observations led Kitaigorodskii et al. to conclude that the wave number expression (Equation 2) was the valid scaling for both the deepwater and the shallow-water wind wave equilibrium ranges. This has been confirmed by other investigators (Gadzhiyev and Kratsitsky 1978, Vincent 1982).

8. Taking the shallow-water limit of the linear wave dispersion relation, i.e.,

$$\lim_{h \rightarrow 0} \left[(2\pi f)^2 = gk \tanh(kh) \right] \quad \text{or} \quad 2\pi f = (gh)^{1/2} k \quad (9)$$

where h is the water depth, it is seen that a k^{-3} dependence is equivalent to an f^{-3} dependence in shallow water. Thus, in frequency notation, the slope of the high frequency side of the nearly saturated wind wave spectrum transforms from an f^{-5} to an f^{-3} during the shoaling process for the part of the spectrum that can be described by linear wave theory.

9. Kitaigorodskii et al. (1975) developed a frequency dependent factor $\Phi(2\pi f, h)$ to transform the f^{-5} deepwater range factor $E_m(f)$ to its finite depth water equivalent, resulting in the following expression for the finite water depth equilibrium range:

$$\begin{aligned} E_m(f, h) &= E_m(f) \cdot \Phi(2\pi f, h) \\ &= \alpha g^2 f^{-5} (2\pi)^{-4} \cdot \Phi(2\pi f, h) \end{aligned} \quad (10)$$

where

$$\Phi(2\pi f, h) = \left[\frac{k^{-3}(\omega, h) \frac{\partial k(\omega, h)}{\partial \omega}}{k^{-3}(\omega, \infty) \frac{\partial k(\omega, \infty)}{\partial \omega}} \right] \quad (11)$$

and $\omega = 2\pi f$.

An iterative expression arises for $\Phi(2\pi f, h)$ when linear wave theory is used in Equation 11. One form is given by

$$\Phi(2\pi f, h) = [R(\omega_h)]^{-2} \cdot \left\{ 1 + \frac{2\omega_h^2 R(\omega_h)}{\sinh [2\omega_h^2 R(\omega_h)]} \right\}^{-1} \quad (12)$$

with

$$\omega_h = 2\pi f \left(\frac{h}{g} \right)^{1/2} \quad (13)$$

and $R(\omega_h)$ is obtained from the iterative solution of

$$R(\omega_h) \tanh [\omega_h^2 R(\omega_h)] = 1 \quad (14)$$

The function Φ approaches the value of one in deep water and a value of zero as the depth decreases, as shown in Figure 1. A simple approximation for $\Phi(2\pi f, h)$ is given in Thompson and Vincent (1983) as

$$\Phi(2\pi f, h) = \begin{cases} \frac{1}{2} \omega_h^2 & \text{for } \omega_h \leq 1 \\ 1 - \frac{1}{2} (2 - \omega_h)^2 & \text{for } \omega_h > 1 \end{cases} \quad (15)$$

This approximation deviates from Equation 12 by a maximum of 4 percent in the vicinity of $\omega_h = 1.0$ with the error less than 1 percent outside the range $0.8 < \omega_h < 1.3$.

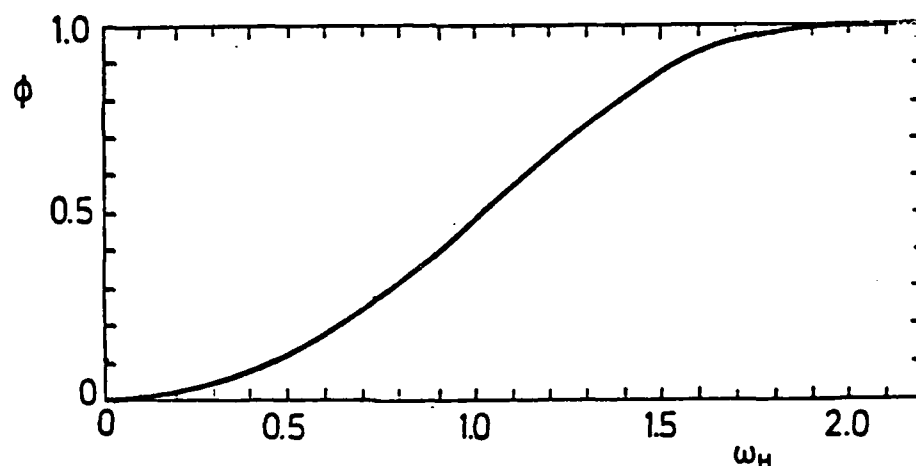


Figure 1. Kitaigorodskii et al.'s Φ as a function of ω_h (Bouws et al. 1985a)

Depth-Limited Significant Wave Height

10. Vincent (1982) pointed out that the estimate of the upper limit on energy density in shallow water, as provided by Equation 10, could be integrated to get total energy if a low-frequency cutoff value is known, i.e.,

$$E = \int_{f_c}^{\infty} \alpha g^2 f^{-5} (2\pi)^{-4} \Phi(2\pi f, h) df \quad (16)$$

For shallow water, when the primary frequency components fall in the range of $\omega_h < 1$, and assuming that $f_c = 0.9f_m$, Equation 16 becomes

$$E = \int_{0.9f_m}^{\infty} \alpha g^2 f^{-5} (2\pi)^{-4} \left(\frac{1}{2} \omega_h^2\right) df = \frac{\alpha g h}{2(2\pi)^2} \int_{0.9f_m}^{\infty} f^{-3} df \quad (17)$$

when Equation 15 is used to approximate $\Phi(2\pi f, h)$. Integrating Equation 17 and applying the limits yields

$$E = \frac{\alpha g h}{4(2\pi)^2 (0.9f_m)^2} \quad (18)$$

Using the energy-based definition for significant wave height,

$$H_{mo} = 4(E)^{1/2} \quad (19)$$

Equation 18 provides an estimate of the depth-limited significant wave height of

$$H_{mo} = \frac{1.1}{\pi} (\alpha g h)^{1/2} T_m \quad (20)$$

where $T_m = 1/f_m$.

11. Initially, α in Equation 20 was taken to be Phillips' constant equal to 0.0081, but more recent results have provided an expression for α which varies according to depth, windspeed, and peak frequency f_m . This will be covered shortly in more detail. Engineering use of Equation 20 should be limited to water depths between the surf zone out to depths where the primary energy-containing frequencies are defined by $\omega_h = 1$.

TMA Spectrum

Self-similar spectral form

12. Bouws et al. (1985a) hypothesized that a first approximation for a finite depth wind sea spectral shape would be obtained simply by substitution of Kitaigorodskii et al.'s expression for the equilibrium range (given by Equation 10) for the deepwater equilibrium range $E_m(f)$ in the JONSWAP Equation (given in Equation 5). They obtained the following:

$$E_{TMA}(f, h) = \alpha g^2 f^{-5} (2\pi)^{-4} \Phi(2\pi f, h) e^{-5/4(f/f_m)^{-4}} \frac{1}{\gamma} \exp \left[-\frac{(f/f_m - 1)^2}{2\sigma^2} \right] \quad (21)$$

with $\Phi(2\pi f, h)$ given by Equation 11.

13. Bouws et al. named their self-similar finite water depth spectral shape the TMA spectrum by combining the first three letters of the three data sets used for field verification (Texel, MARSEN, and ARSLOE), each of which is explained below. Equation 21 has the four JONSWAP parameters, α , γ , f_m , and σ plus the depth h . An example of the finite depth effect of the TMA spectral form is shown in Figure 2 in which all the parameters are held constant except the depth. Figure 3 is the same presentation but plotted in wave number space, which shows the k^{-3} scaling from deep water to shallow water.

Field verification

14. Bouws et al. (1985a) used field data from three separate studies on shallow-water wind wave growth to investigate the parameters used in the TMA spectral representation. MARSEN (the Marine Remote Sensing Experiment at the North Sea) and ARSLOE (the Atlantic Remote Sensing Land-Ocean Experiment) were both comprehensive experiments in which ocean wave measurements were but a part of the entire program. The experimental sites are both on the continental shelf with depths up to 40 m; but the ARSLOE site was open to the Atlantic Ocean, while the MARSEN site was located in the southern half of the North Sea. The Texel data set is comprised of a series of measurements made near the Texel lightship west of Rotterdam during a longlasting northwesterly storm in the central and southern North Sea.

15. The combined data represent conditions with windspeeds ranging between 4 and 25 m/sec, bottom materials ranging from fine to coarse sands, bottom slopes ranging from 1:150 to nearly flat, and depths from about 5 m

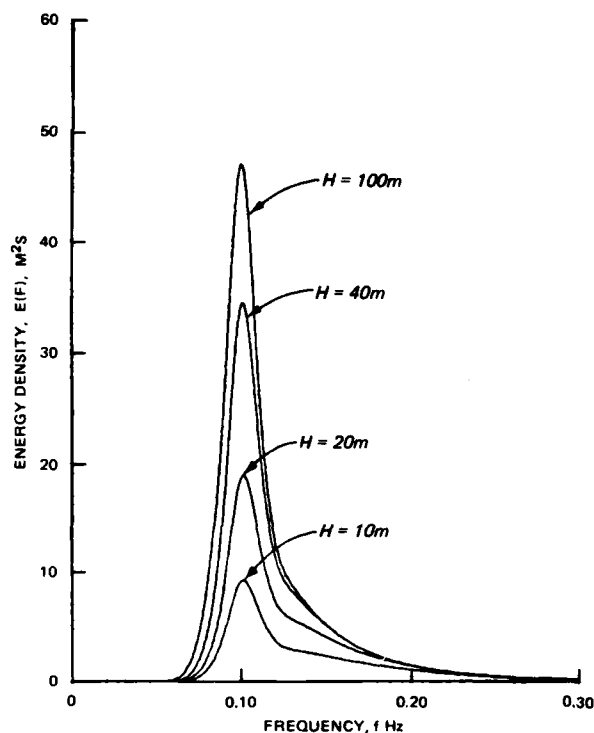


Figure 2. A family of wind wave spectra with identical JONSWAP parameters in frequency space (TMA spectral form)

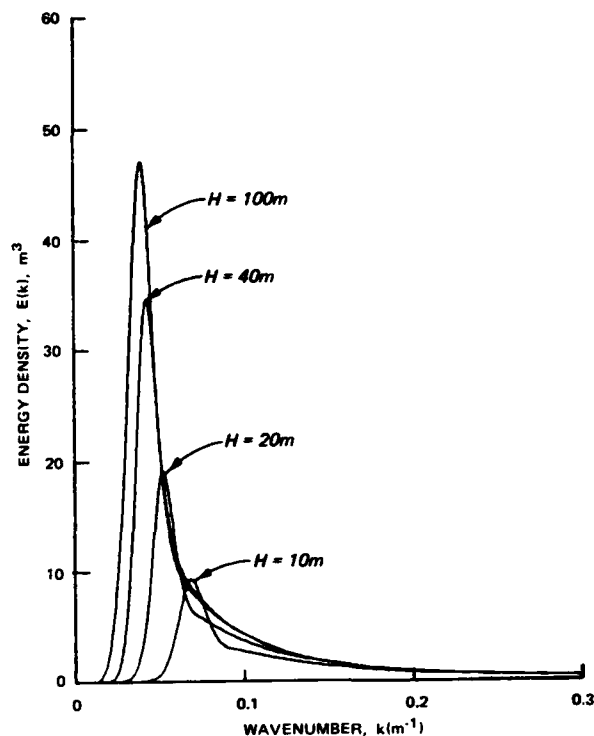


Figure 3. A family of wind wave spectra with identical JONSWAP parameters in wave number space (TMA spectral form)

to 45 m. An extensive description of the data set is given in Bouws et al. (1985a).

16. Bouws et al. (1985a) fitted the TMA spectral form to over 2,800 wind sea spectra to test its viability and to determine if any parametric relationships could be established linking the spectral parameters to the external wind field. In general the fit of the spectrum was of the same quality as the fit of the JONSWAP spectrum to deepwater wind sea spectra. Examples of the fit to field spectra are given in Figure 4.

TMA parametric relationships

17. The relationships between the TMA spectral parameters and various dimensionless quantities such as dimensionless peak frequency and wave number were examined by Bouws et al. (1985a). They determined that α and γ could be expressed by the following empirical expressions for all water depths:

$$\alpha = 0.0078k^{0.49} \quad (22)$$

$$\gamma = 2.47k^{0.39} \quad (23)$$

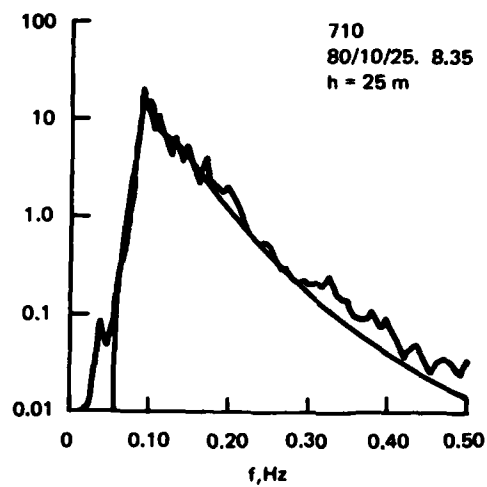
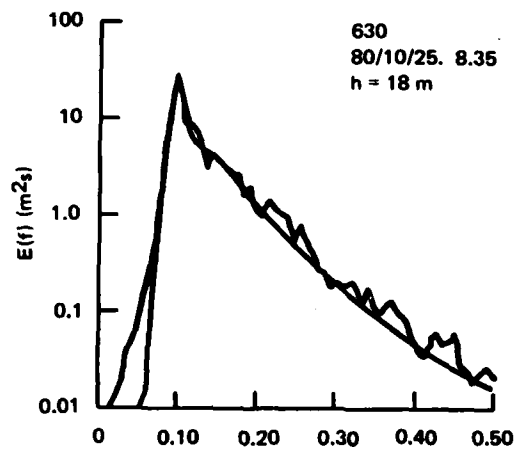
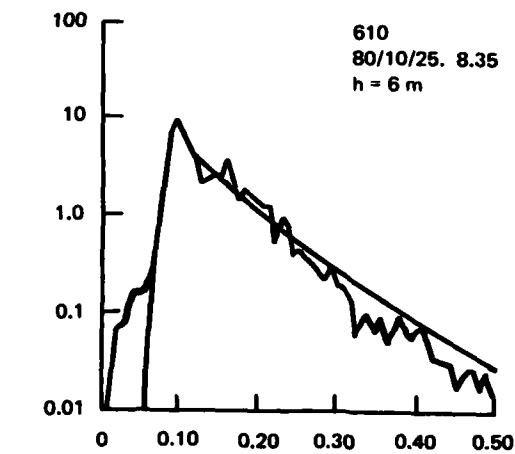


Figure 4. TMA spectra fit to field data
from ARSLOE data set

where

$$\kappa = \frac{U^2}{g} k_m \quad (24)$$

with

U = windspeed at 10 m elevation

g = acceleration of gravity

$k_m = 2\pi/L_m$ = wave number for waves at peak frequency

L_m = wavelength associated with peak frequency f_m from linear wave theory

Examination of the variation of σ in the fitting of the spectra to the TMA representation gave no statistical correlation, so it was suggested that the mean values of

$$\sigma = \begin{cases} \sigma_a = 0.07 & f \leq f_m \\ \sigma_b = 0.09 & f > f_m \end{cases} \quad (25)$$

are sufficient when using the TMA spectrum.

18. A certain amount of scatter was present in the plots from which the parametric relationships were derived. Bouws et al. (1985b) demonstrated that the scatter could be simulated by assuming that the error in determination of windspeed was normally distributed with a standard deviation between 10 and 20 percent. They concluded that the methods used to determine windspeed could easily contain errors on that order. The most remarkable consequences of the TMA research were (a) showing that the effect of depth could be incorporated solely through the dependence of κ on depth, and (b) determining that there was no apparent systematic dependence on bottom type.

19. The preceding equations provide a means of predicting the limiting wind sea spectral shape in finite depth waters in terms of the windspeed and the peak frequency. The procedure is to determine κ from Equation 24, find α and γ (Equations 22 and 23, respectively), and then calculate $E_{TMA}(f, h)$ values using Equation 21. The Φ function is determined for each frequency using either Equation 12 or (if a slightly less accurate answer can be tolerated) Equation 15. Significant wave height can be determined by numerically integrating the resulting shallow-water spectrum and then applying the relationship for H_{mo} given by Equation 19, but an easier approach is to use Vincent's depth-limited significant wave height expression given by

Equation 20, provided that $w_h < 1$ for most of the energy containing frequencies.

TMA internal parameterizations

20. Starting with Kitaigorodskii et al.'s (1975) basic equation for the equilibrium range (Equation 2), Vincent (1985a) was able to derive an expression for α in terms of significant wave steepness ϵ . This expression is the following:

$$\alpha = 16\pi^2 \epsilon^2 \quad (26)$$

where

$$\epsilon = \text{significant wave steepness} = E^{1/2}/L_m \quad (27)$$

E = total energy in the spectrum

L_m = wavelength associated with f_m as defined in linear theory

This result is identical with that obtained by Huang et al. (1981) for a JONSWAP spectrum in deep water. Field data support Vincent's formulation; thus, Equation 26 holds for all water depths.

21. Equating Equation 26 and Equation 22 gives an expression for κ in terms of ϵ which can then be put into Equation 23 to yield

$$\gamma = 6614\epsilon^{1.59} \quad (28)$$

which should be valid for wind seas. The main advantage of this internal parameterization is the ability to specify the equilibrium wind sea spectrum associated with a given energy level.

22. It is an interesting exercise to show that Vincent's depth-limited significant wave height equation (Equation 20) and the expression for α (Equation 26) are the same. The energy E in Equation 27 can be given in terms of H_{mo} from the relationship of Equation 19. Substitution into Equation 26 yields

$$H_{mo} = \frac{1}{\pi} (\alpha)^{1/2} L_m \quad (29)$$

and taking $L_m = (gh)^{1/2} T_m$ in shallow water gives

$$H_{mo} = \frac{1}{\pi} (\alpha gh)^{1/2} T_m \quad (30)$$

The only difference between Equation 30 and Equation 20 is the 1.1 factor which Vincent (1982) arrived at by assuming a cutoff frequency of $0.9 f_m$. Equation 29 is a more general form of Equation 30, and it can be applied throughout the shallow- and intermediate-water depth ranges when the appropriate expression for L_m is used and α is found from Equation 22.

23. To reiterate, significant wave heights H_{mo} found using either Equation 29 or Equation 30 are the maximum values that can occur at that depth for the given values of peak period and windspeed. In addition, H_{mo} calculated for very shallow water can be substantially less than the significant wave height H_s defined as the average of the highest 1/3 waves. H_{mo} provides an estimate of the energy contained in the wave spectrum, while H_s provides a statistical estimation of the wave heights. This variation in shallow water is due to the increasing nonlinearity in the waves. A full treatment of this topic is provided in Thompson and Vincent (1985), and provision is made for this effect in a later section of this report.

24. Since Equation 29 reduces to Vincent's depth-limited result in shallow water, it might be suspected that a similar exercise could be performed for deep water. Replacing L_m in Equation 29 with the deepwater relationship, $L_{mo} = (g/2\pi)T_m^2$, replacing α with Equation 22, and nondimensionalizing results in

$$\frac{gH_{mo}}{U^2} = 0.0112 \left(\frac{gT_m}{U} \right)^{3/2} \quad (31)$$

when the exponent of κ in Equation 22 is taken as 1/2. A similar result is found if the deepwater fetch-limited equations for wave height and wave period in the Shore Protection Manual (SPM) (1984) are combined, the only difference being a coefficient of 0.0105 instead of 0.0112.

25. The expression for the fully developed wind sea significant wave height in deep water can now be derived by replacing T_m in Equation 31 with the fully developed wave period as defined in Equation 4. This results in

$$\frac{gH_{mo}}{U^2} = 0.238 \quad (32)$$

The only difference between Equation 32 and the expression for fully developed deep water H_{mo} given in the SPM (1984) is the value of 0.243 instead of 0.238. This is remarkable because the SPM equation was arrived at by

consideration of the time necessary to reach full development of the JONSWAP equations.

26. This exercise has illustrated that the internal and external parameterizations for α can be applied for all water depths outside of the surf zone. The ability to recover deepwater results is particularly interesting since the parameterization of α as a function of f_m and windspeed was done using data largely from shallow- and intermediate-water depths.

Wave Growth Limitation

Wave period limit

27. Vincent and Hughes (1985) examined the question of whether or not finite depth wind waves reach a fully developed state where the peak spectral frequency becomes fixed and no longer migrates toward lower frequencies, regardless of the energy input. Evidence that such a cutoff frequency may exist comes from the Lake Okeechobee and the Gulf of Mexico data used by Bretschneider (1958) to develop shallow-water wave growth curves. Bretschneider plotted gT_m/U versus gh/U^2 and determined an empirical relationship for the cutoff frequency in shallow water. Vincent and Hughes pointed out that the quenching of atmospheric input of energy, which occurs in deep water when the celerity of the waves exceed the windspeed, did not appear to occur in shallow water. This is because at a given depth all waves of frequency less than f^* have the same celerity, if f^* is the highest frequency where the shallow-water dispersion relation is a valid approximation. If the deepwater growth mechanism is assumed, it would be possible to have windspeeds in excess of the wave speed and still have wave growth.

28. Vincent and Hughes (1985) proposed that the cutoff frequency where shallow-water wave growth would stop should be determined by a frequency where the shallow-water dispersion relation held plus a further shift to slightly lower frequencies due to resonant wave-wave interactions. This frequency is defined as

$$\omega_{hm} = 2\pi f_m \left(\frac{h}{g} \right)^{1/2} = 0.9 \quad (33)$$

and it arises from Kitaigorodskii et al.'s (1975) observation that the transition from a deepwater f^{-5} equilibrium range to an f^{-3} range for

shallow-water waves occurred when $\omega_h \approx 1$. The slight downward shift in frequency is empirically represented by the 0.9 value.

29. Rearranging Equation 33, multiplying by g/U and noting $T_m = 1/f_m$, the following nondimensional expression results which may be compared to Bretschneider's result:

$$\frac{gT_m}{U} = \frac{2\pi}{0.9} \left(\frac{gh}{U^2} \right)^{1/2} \quad (34)$$

This comparison is made in Figure 5, and it demonstrates a reasonable fit to the field data. The advantage of Equation 33 is that a value of windspeed is not a factor in determining the fully developed cutoff frequency in shallow water. In other words, it is assumed that once a fully developed condition exists in shallow water, the peak frequency remains fixed regardless of any increase in windspeed.

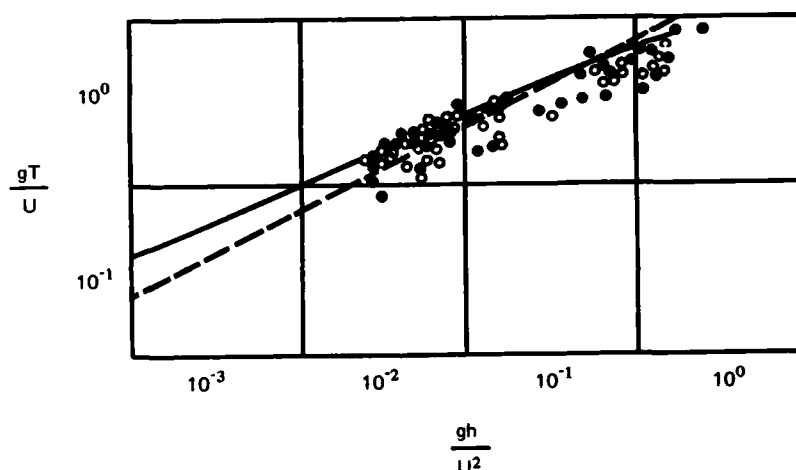


Figure 5. Relationship between dimensionless period and depth (dashed line is Equation 34; solid line is Bretschneider's (1958) empirical fit) (Vincent and Hughes 1985)

Wave height limit

30. Bretschneider (1958) also presented nondimensional significant wave height versus nondimensional depth for the shallow-water fully developed data. Vincent and Hughes (1985) were able to show that Vincent's estimate for depth-limited significant wave height (Equation 20) can be used to derive an expression for the fully developed case closely matching Bretschneider's empirical formulation. They expressed k_m in Equation 24 as

$$k_m = \frac{2\pi}{L_m} = \frac{2\pi}{(gh)^{1/2} T_m} = \frac{0.9}{h}$$

where L_m is replaced by its shallow-water expression from linear theory and T_m is found from Equation 33 for the fully developed case. Using this expression for k_m , the value of α for the fully developed case is determined from Equation 22 as

$$\alpha = 0.0074U/(gh)^{1/2} \quad (35)$$

where the 0.49 exponent of Equation 22 is taken as 1/2. Substituting Equation 35 for α and Equation 33 for T_m into Equation 20 yields

$$H_\ell = \frac{0.210U^{1/2}h^{3/4}}{g^{1/4}} \quad (36)$$

where H_ℓ is the significant wave height for the fully developed case. Non-dimensionalizing by g/U^2 gives

$$\frac{gH_\ell}{U^2} = 0.210 \left(\frac{gh}{U^2} \right)^{3/4} \quad (37)$$

Equation 37 is compared to Bretschneider's result in Figure 6.

31. The favorable fit of the equations for fully developed wave period and wave height to the shallow-water field data of Bretschneider lend support to the TMA shallow-water self-similar spectral form and to the parameterizations made for α . However, there are still many unanswered questions involving the underlying physical processes which result in the TMA spectrum. It must be noted that these shallow-water limitations are for full development on a flat bottom, but they do provide a useful upper limit for some engineering purposes.

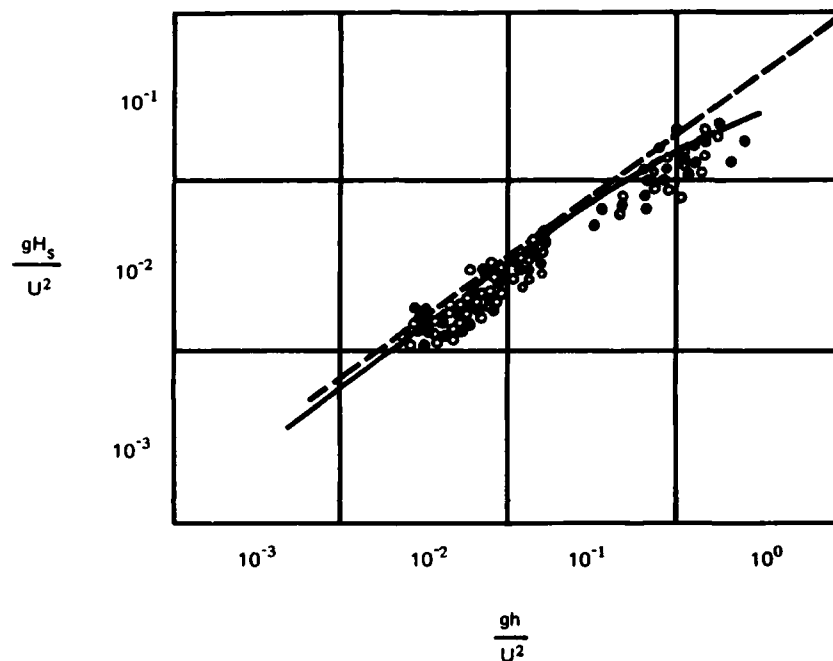


Figure 6. Relationship between dimensionless wave height and depth (dashed line is Equation 37; solid line is Bretschneider's (1958) empirical fit (Vincent and Hughes 1985))

PART III: SURF ZONE SPECTRA

32. In the formulation and parameterization of the TMA spectral form by Bouws et al. (1985a) the data examined were restricted to those spectra recorded outside of the surf zone. They were uncertain of the appropriateness of using linear wave theory in the surf zone to convert from wave number space to frequency space via Kitaigorodskii et al.'s (1975) Φ function. Also, outside the surf zone the balance of forces determining spectral evolution are comprised of wind, breaking (largely at high frequencies), dissipation due to a bottom boundary layer, and transfers of energy in the spectrum. Once the surf zone is reached, major breaking occurs near the peak of the spectrum thus introducing a separate concern. Vincent examined the fit of the TMA spectral form to spectra collected well within the surf zone during the ARSLOE experiment. (The surf zone spectra were not a part of the ARSLOE portion of the data set used to determine the TMA parameters).*

Fit of TMA to Collected Spectra

33. The TMA form was fitted to the spectra only over the region up to twice the spectral peak frequency $2f_m$. Beyond this frequency forced harmonics begin to dominate the spectrum, while the TMA form is meant to represent only free wave energy. Figure 7 is an example of the best fit obtained by Vincent to a surf zone spectrum recorded in 1.7 m of water. A reasonable fit is made between the range of $0.5f_m$ to $2.0f_m$, which is the principal energy containing region. At higher frequencies the TMA form underestimates the energy content. Vincent (1985b) noted that the energy contained at these higher frequencies increases as the depth decreases. This increased energy represents the increasing nonlinearity of the long period wave components in shallow water. Vincent suggested a modifying factor for the TMA spectral form, but he lacked the necessary data to provide a generally applicable modification. However, as a first approximation, the unmodified TMA spectrum can be used to represent surf zone spectra if the spectral parameters can be estimated. The resulting estimated significant wave height found using this approach was within 10 percent of the actual values for the cases that Vincent examined.

* Personal correspondence between Vincent and Hughes, January 1984.

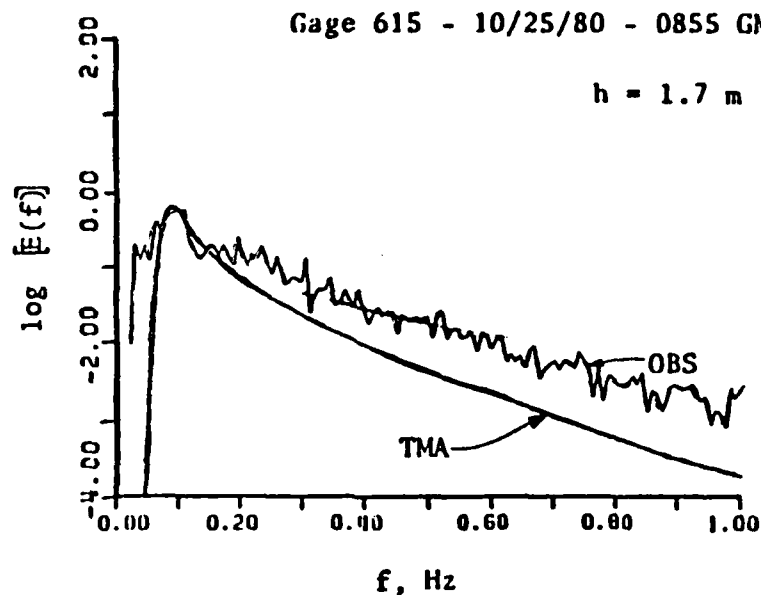


Figure 7. Fit of TMA spectrum to surf zone irregular wave spectrum

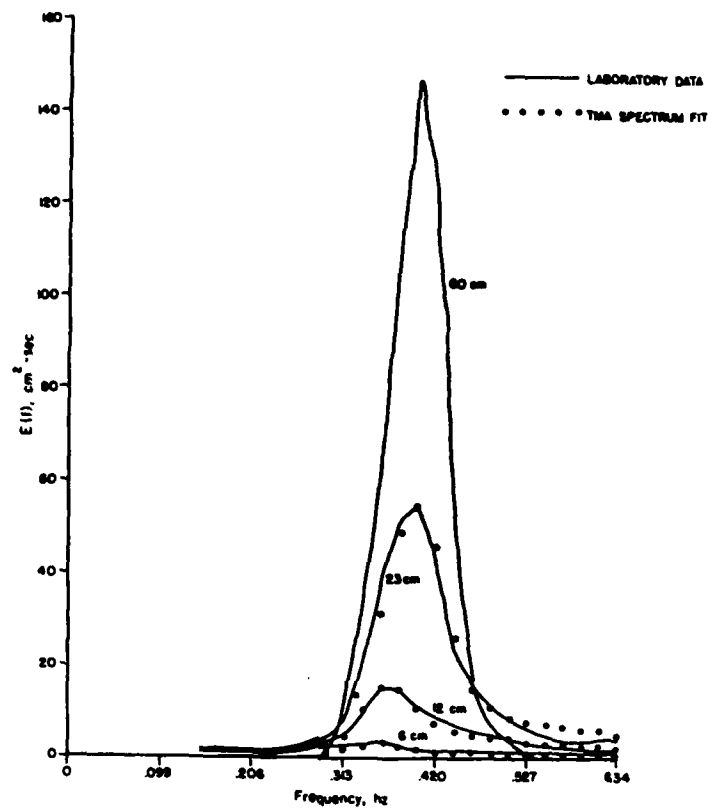
Note that the logarithmic scale for energy density used in Figure 7 makes it appear that the difference in total energy between the TMA fit and the actual spectrum is greater than it truly is.)

34. An unexpected result of this work was the reasonable fit of the TMA spectral form to broad swell spectra in the surf zone obtained from both the field and the laboratory. This is surprising for two reasons. First, the broad swell is more indicative of a decaying than a growing sea state for which the self-similar spectrum was proposed. Second, there is no reason to expect that mechanically generated irregular waves in the laboratory should follow the TMA form for wind waves since the primary forcing function (the wind) is absent. This latter observation was found to be true for both characteristic broad swell spectra outside the surf zone as well as for typical wind sea spectra simulated in the laboratory. Figure 8 illustrates the fitting of the TMA spectral form to laboratory data shoaled over a 1:30 slope.

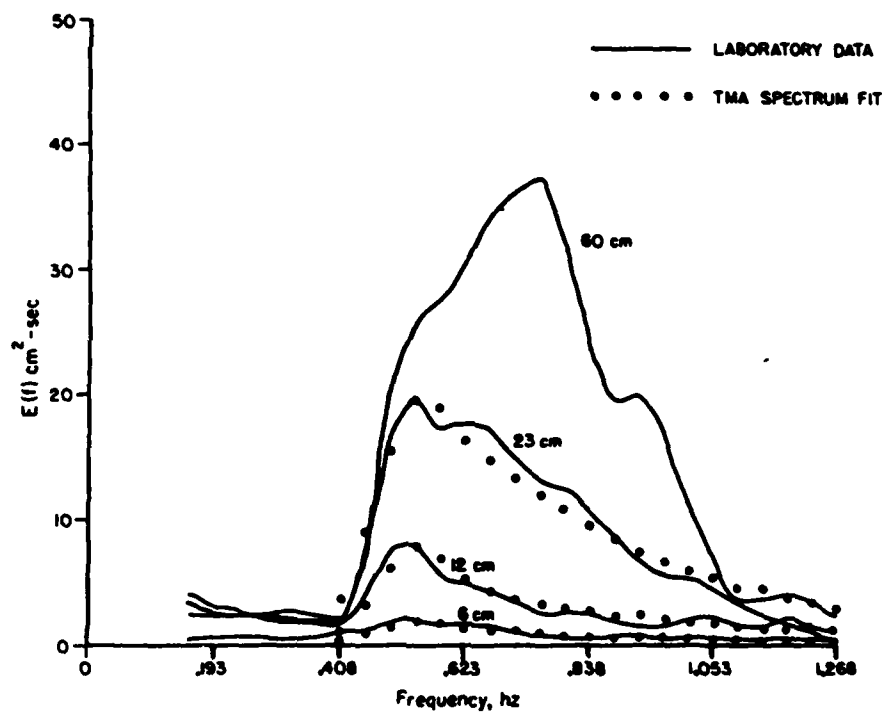
Hypothesis for Energy Saturation

Local saturation zone

35. Vincent (1985b), suggested a hypothesis for energy saturation of irregular waves during shoaling by proposing a separation of the saturation process during shoaling into two distinct types: the local and universal



a. Spectrum typical of swell



b. Spectrum typical of wind seas

Figure 8. Fit of the TMA spectrum to laboratory data on 1:30 slope (Vincent 1985b)

saturation zones. As waves progress into finite depth waters, they first enter a local saturation zone in the intermediate and shallow-water depths where nonlinear wave-wave interactions shift energy away from the principal energy containing frequencies to higher frequencies where it is dissipated by deepwater breaking mechanisms. This is the region for which all the previous TMA formulations and parameterizations for wind waves are valid. It appears that broad swell spectra also can be fitted by the TMA form in this region, but there is no external parameterization for α in this case.

Universal saturation zone

36. Eventually, if the water depth becomes sufficiently shallow, wave breaking begins to occur at the peak of the spectrum, and dissipation dominates the spectrum. Vincent (1985b) referred to this region as the universal saturation zone. While there still may be some transfer of energy between frequencies in this zone, the wave train is basically a series of nondispersive waves, each breaking in sequence. The fact that the TMA spectral form could be fitted to data gathered within the surf zone indicated to Vincent that the spectral parameters could be obtained from the steepness equations (Equations 26 and 28) if a saturated value for the energy could be obtained. Working on the hypothesis that the largest wave at a given depth in the universal saturation zone is controlled by the depth, Vincent (1985b) proposed

$$H_{mo} = Bh \quad (38)$$

where

$$h = \text{water depth} \quad (39)$$

$$B = \frac{R_{max}}{R_{so} R_{ms}}$$

and

$$R_{max} = H_{max}/h \quad \text{for monochromatic waves}$$

$$R_{so} = H_s/H_{mo}$$

where

$$H_s = \text{average of the highest 1/3 waves}$$

$$R_{ms} = H_{max}/H_s \simeq 1.33$$

Values for R_{\max} can be obtained from Figure 9, which is reproduced from the SPM (1984), and values for R_{so} can be found from the "average" line in Figure 10, which is reproduced from Thompson and Vincent (1985). For slopes typical of most beaches, the coefficient B ranges between 0.55 and 0.65. These values are consistent with the value of $B = 0.6$ suggested by Thornton and Guza (1982), and unless the area of concern varies greatly from a "typical" beach, the value of 0.6 for B is probably sufficient for engineering purposes. The significant steepness is found from Equation 27 as

$$\varepsilon = \frac{(E)^{1/2}}{L_m} = \frac{H_{mo}}{4L_m} = \frac{Bh}{4(gh)^{1/2}T_m} \quad (40)$$

when Equation 19 is used for H_{mo} and the linear theory shallow-water wavelength is substituted. The parameter α can now be found from Equation 26

$$\alpha = \frac{\pi^2 B^2 h f_m^2}{g} = \left(\frac{B\omega_{hm}}{2} \right)^2 \quad (41)$$

where

$$\omega_{hm} = 2\pi f_m \left(\frac{h}{g} \right)^{1/2} \quad (42)$$

37. The ability of Equation 41 to predict α in very shallow water is shown in Figure 11 (from Vincent 1984). The figure shows reasonable agreement for both laboratory and field data in the universal saturation zone. Note that in the universal saturation zone H_{mo} varies linearly with depth (Equation 38), while in the local saturation zone H_{mo} varies with the square root of the depth (Equation 20). Also note that the equation for H_{mo} in the local saturation zone (Equation 20) reduces to the expression for H_{mo} in the universal saturation zone (Equation 38) when Equation 41 is substituted for α . This is not surprising since both equations are linked to the equation for α in terms of ε .

38. It is somewhat difficult to define a demarcation line between the local saturation zone and the universal saturation zone. Ideally there should be some limiting value of significant steepness beyond which wave breaking at the spectral peak is assured.

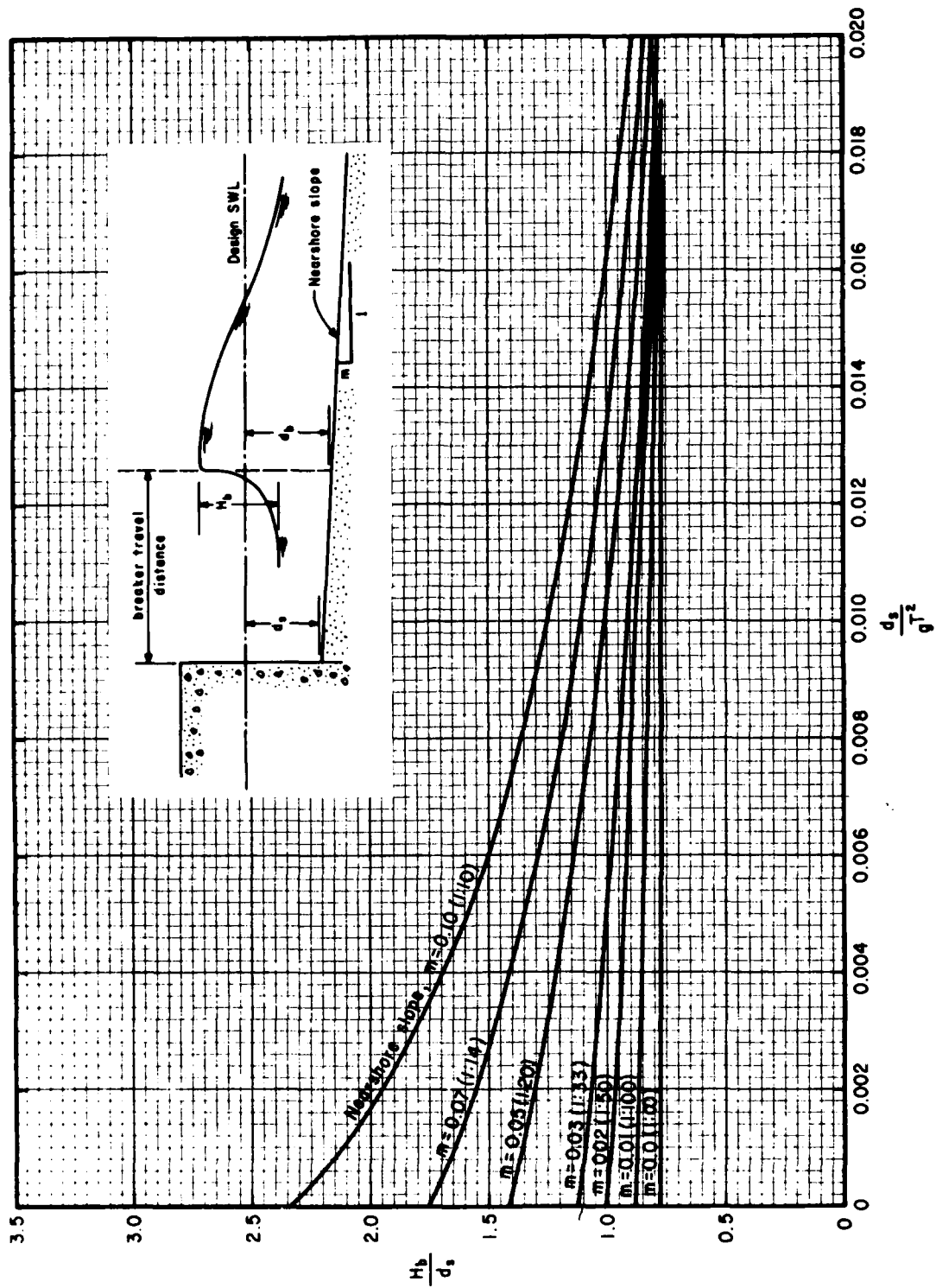


Figure 9. Dimensionless breaker height versus relative depth (from SPM 1984)

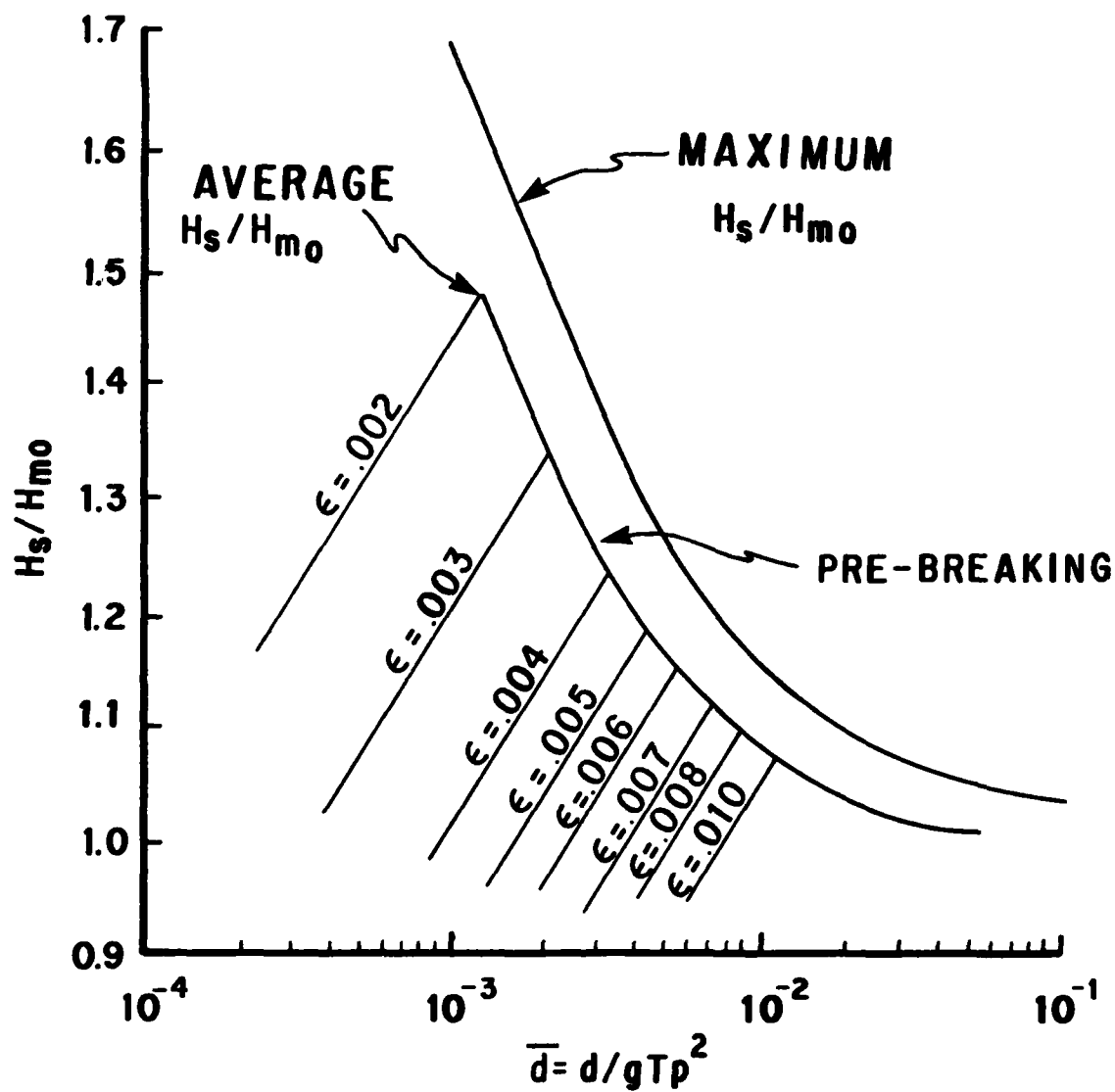


Figure 10. Maximum and average values of H_s/H_{m0} for irregular waves
(from Thompson and Vincent 1985)

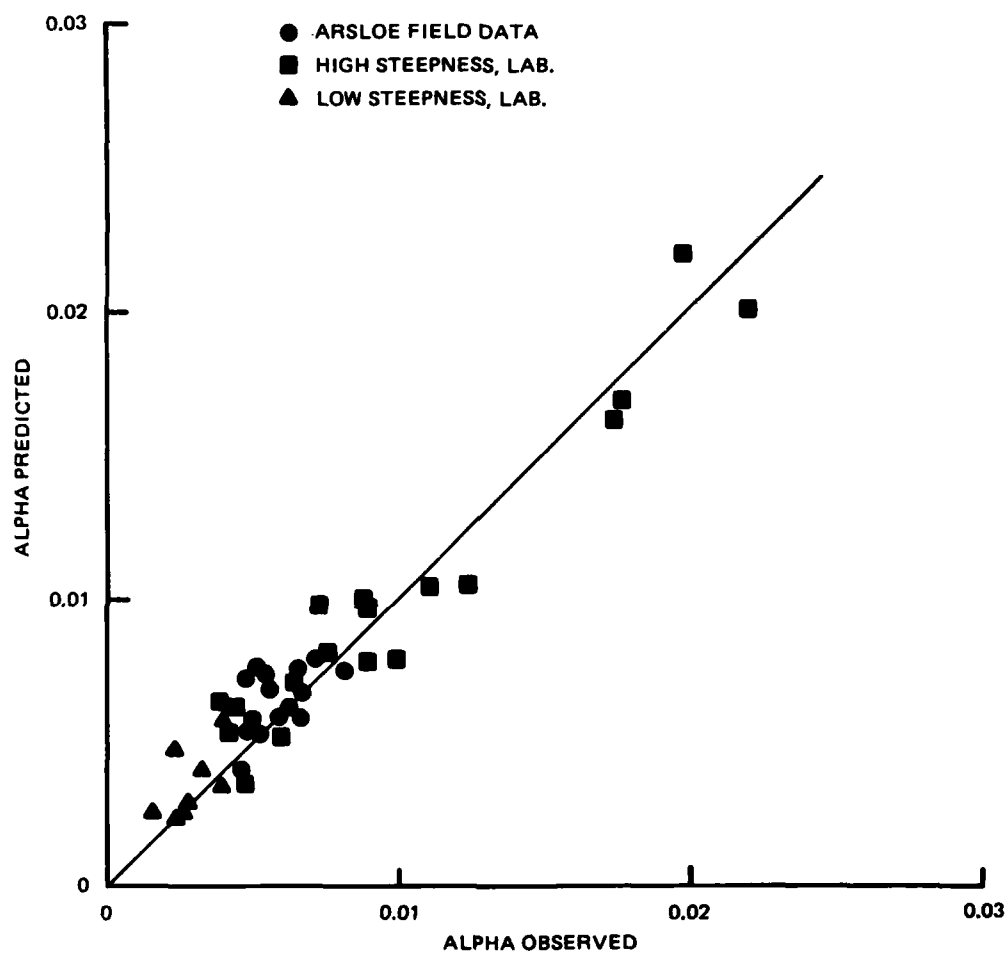


Figure 11. Alpha predicted versus alpha observed (from Vincent 1984)

PART IV: DISCUSSION

39. Thus far the focus of this report has been on past developments in the specification of self-similar spectral forms and their role in the development of the new TMA spectral form. By adding more and more terms to Phillips' (1958) representation of the limiting energy density in the equilibrium range, researchers progressively specified a self-similar spectral shape for deep water (Pierson-Moskowitz), a fetch-limited deepwater spectrum (JONSWAP), a shallow-water equilibrium range (Kitaigorodskii et al.), and finally a self-similar equilibrium spectral form valid at all water depths (TMA).

40. The self-similar parametric TMA representation was shown to have the ability to represent wind waves and broad swell, and it appears that both the deepwater and shallow-water limits merge with previously obtained empirical results. It was seen also that the TMA form even fit very shallow surf zone spectra up to twice the peak frequency.

Physical Implications of the TMA Spectral Form

41. The fact that the self-similar TMA form can describe wind sea spectra in deep, intermediate, or shallow water reinforces the conclusion of Kitaigorodskii et al. (1975) that the basic scaling lies in k -space rather than in frequency space. Also, the linear theory dispersion relation seems adequate for converting from wave number space to frequency space via the ϕ factor.

42. Both the JONSWAP and the TMA spectral forms extended the k^{-3} scaling for the equilibrium range across the entire spectrum. There is no physical explanation as to why this scaling should be valid, but years of experience using the JONSWAP form, coupled with the relative good fit of the TMA form to shallow-water spectra, indicates that the scaling does hold outside the equilibrium range.

43. Self-similarity in spectral form implies that there is a relative balance between the wind energy input, energy transfers within the spectrum, and energy dissipation. This balance is maintained and limited to produce a consistent spectral shape. No analyses have been made into the very difficult problem of the spectral balance between the various source/sink terms such as nonlinear wave-wave interactions, wave dissipation, atmospheric input, bottom

friction, percolation, etc., for the TMA data set. However, it is tentatively concluded that the bottom friction effect in the dissipation of wave energy is substantially less than originally thought. This conclusion is based on the observation that the parametric relationships provide equally good spectral approximations over a wide variety of depths and bottom materials. Thus it is unlikely that bottom dissipation would be a dominant influence on spectral shape. With the establishment of the TMA shape, study into the various source/sink terms now can be restricted to combinations which will produce a self-similar shape. Bottom friction for typical beaches is thought to be more important for swell than for wind seas.

44. Kitaigorodskii et al.'s (1975) equilibrium range was intended for the case of a horizontal bottom, but the parameterization and application of the TMA spectrum to data from gently sloping bottoms up to slopes of 1:100 indicate that the self-similar equilibrium form evolves rapidly enough to adequately describe the spectral transformation over gentle slopes. Steep sloped beaches might not permit the equilibrium condition to be reached; hence, the TMA spectrum could well represent an unattainable limit on a steep slope.

45. Vincent (1985b) sums up the TMA spectral form as "...a quantitative description of the wave transformation process with a useful parameterization scheme." He adds that while many of the principal physical processes occurring in wave shoaling have been identified, a deterministic description is still in the future.

Assumptions and Limitations of the TMA Spectral Form

46. The primary underlying assumption invoked when applying the TMA spectrum and the prognostic equations is that the wind sea is at a steady state or equilibrium condition. This means that the wind has been steady long enough (as yet undefined) for the waves to reach equilibrium and that the bottom topography is a gentle slope with smoothly varying features and without complexities which might cause rapid alteration of the wave train. Until further data are examined, a slope steepness guideline of 1:100 is suggested which arises from the limit of the TMA data set. While steeper slopes might be able to maintain the TMA equilibrium condition, the worst that can happen by using the TMA approximation on a steep slope is a conservative estimate of the maximum possible significant wave height for the given conditions. Note

that laboratory data on a 1:30 slope were adequately described using the TMA representation.

47. The TMA spectrum as it is presently parameterized cannot be used in fetch- or duration-limited shallow-water wave growth situations since it is a final steady state form. Fetch- or duration-limited design in shallow water needs to be conducted using numerical models (for complex regions) or wave forecasting curves such as provided in ETL 1110-2-305 (Vincent and Lockhart 1984). Future developments will probably provide a TMA fetch- and duration-limited form paralleling the deepwater JONSWAP equations.

48. The TMA spectral form is for a single-peaked spectrum containing only minor low-frequency energy. In most instances large wave conditions will result from either a local storm or swell resulting from a nearby storm. These spectra will probably propagate toward shore as a single-peaked spectrum describable by the TMA shape. The TMA formulation does not handle multi-peaked spectra which, according to Thompson (1980), constitute over 60 percent of the coastal wave conditions in the United States. However, most of the multi-peaked cases are of low energy and of minor importance for engineering design. The TMA shape may be used to describe the individual spectral peaks.

49. The shallow-water limits to wave growth derived as a cutoff frequency and a limiting significant wave height fit the field data and provide useful engineering guidance. The limits are strictly for full development over a horizontal bottom or a gently sloping bottom.

50. The TMA prognostic equations require specifications of either (a) U , h , and f_m , or (b) $\varepsilon = f(H_{mo}, h, \text{ and } f_m)$. Vincent (1984) suggests that when wave conditions are steady and the combination of beach slope and propagation distance are sufficiently small, then f_m may be projected from deep water into shallow water. In other words, the peak frequency doesn't shift during shoaling. Field data from two 1980 storms at Duck, North Carolina, indicated that f_m did not change more than 10 percent over a 36 km distance in which the depth changed from 36 to 2 m. In cases where wind fields and bottom conditions are highly inhomogeneous and f_m is expected to shift, a fully time-dependent spectral model is needed to determine f_m in shallow water.

PART V: ENGINEERING APPLICATIONS

51. The preceding formulations for a self-similar equilibrium spectrum for all water depths can provide useful engineering design guidance because the equilibrium spectrum puts constraints on the expected energy levels and spectral shapes under given conditions. While it is impossible to list every conceivable application of the TMA spectrum, the following short examples illustrate several engineering uses.

Numerical Models

52. Some of the current shallow-water wave growth and propagation numerical models can simulate wave propagation over complex bathymetry during unsteady wind conditions. These models typically contain many source/sink terms, some of which can be quite site specific. In some applications it is possible for the models to give exaggerated results because there is no effective upper limit to the wave growth. This can be corrected by constraining the numerical simulation to an upper limit of growth on the high frequency side of the spectral peak as defined by the TMA spectrum.

53. Oceanographers at CERC illustrated the usefulness of the TMA spectral form as an upper limit when they modified an existing numerical wave growth spectral model and ran several simulations, with and without the TMA prescribed limit. Generally, it was found that this particular numerical model yielded unrealistically high results for high windspeeds and for beach slopes of 1:200. In other words, sufficient energy dissipation through bottom friction and other sink terms did not occur. When the slope was very mild (1:2,000), bottom friction attenuated the waves adequately. Incorporating the TMA limiting spectral form into the numerical model has made it a better engineering tool; however, this does not relieve the engineer from responsible calibration and verification of the model.

Design Example 1

Given

54. For a smoothly varying bottom slope, construct a set of design curves showing the depth-limited significant wave height H_{mo} as a function

of peak spectral period T_m and windspeed U . The given water depth is 5 m (16 ft).

Solution

55. It is first necessary to choose the proper equation for H_{mo} (either Equation 29 or 30). This is done by determining the wave frequency where $\omega_h = 1$, i.e.,

$$\omega_h = 2\pi f' (h/g)^{1/2} = 1$$

or

$$f' = (9.81/5)^{1/2}/2\pi = 0.22 \text{ Hz}$$

which is $T' \approx 4.5$ sec. When the principal energy containing frequencies have periods greater than 4.5 sec, Equation 30 can be used. We will assume that $f' \approx 1.5 f_m$ or $T_m = 1.5 T' = 6.75$ sec. Any calculations made for peak periods less than 6.75 sec should be done using Equation 29 with L_m being determined using the intermediate depth linear dispersion relation. The calculations are done as follows:

For $U = 10$ m/sec (32.8 ft/sec) and $T_m = 10$ sec, first find

$$L_m = (gh)^{1/2} T_m = [(9.81)(5)]^{1/2} (10) = 70 \text{ m (230 ft)}$$

Next find κ from Equation 24.

$$\kappa = \frac{U^2 2\pi}{gL_m} = \frac{(10)^2 (2\pi)}{(9.81)(70)} = 0.915$$

56. Using Equation 22,

$$\alpha = 0.0078 \kappa^{0.49} = 0.0078 (0.915)^{0.49} = 0.00747$$

and the H_{mo} associated with this T_m and U is by Equation 30

$$H_{mo} = \frac{1}{\pi} (\alpha gh)^{1/2} T_m = \frac{1}{\pi} [(0.00747)(9.81)(5)]^{1/2} \cdot (10) = 1.93 \text{ m (6.3 ft)}$$

To be slightly conservative (10 percent), use the 1.1 factor as given in Vincent's original derivation (Equation 20) to finally arrive at

$$H_{mo} = 1.1 (1.93) = 2.1 \text{ m (6.9 ft)}$$

A simple programming of these few steps supplied the repetitive calculations necessary to produce the set of curves given in Figure 12 for the stated initial conditions. The region of breaking is given by Equation 38 as

$$H_{mo} = Bh = 0.6 (5 \text{ m}) = 3.0 \text{ m}$$

Design Example 2

Given

57. To determine crest elevation for some structures where limited overtopping is allowable, engineers should use the following wave statistics: H_s (average of the highest 1/3 waves), $H_{10\%}$ (average of the highest 10 percent of all waves), and $H_{1\%}$ (average of the highest 1 percent of all waves). They should then calculate these values for a windspeed of 10 m/sec (32.8 ft/sec) and a peak period of 10 sec in a water depth of 5 m (16.4 ft). (Note that these are the same values used in the sample calculation of Example 1.)

Solution

58. From Example 1 it is seen that the given values result in $H_{mo} = 2.1 \text{ m (6.9 ft)}$. First determine if this is a breaking condition as defined by $H_{mo} = Bh$ when $B = 0.6$, i.e.,

$$H_{mo(\text{break})} = 0.6 (5 \text{ m}) = 3.0 \text{ m}$$

Since $H_{mo} = 2.1 \text{ m}$ is nonbreaking, we can determine H_s from Figure 10 using the "average H_s/H_{mo} " curve for a value of relative depth

$$\bar{d} = \frac{h}{gT_m^2} = \frac{(5)}{(9.81)(10)^2} = 0.005$$

The ratio from Figure 10 is about 1.18, therefore H_s becomes

$$H_s = 1.18H_{mo} = 1.18(2.1 \text{ m}) = 2.48 \text{ m (round off to 2.5 m) (8.1 ft)}$$

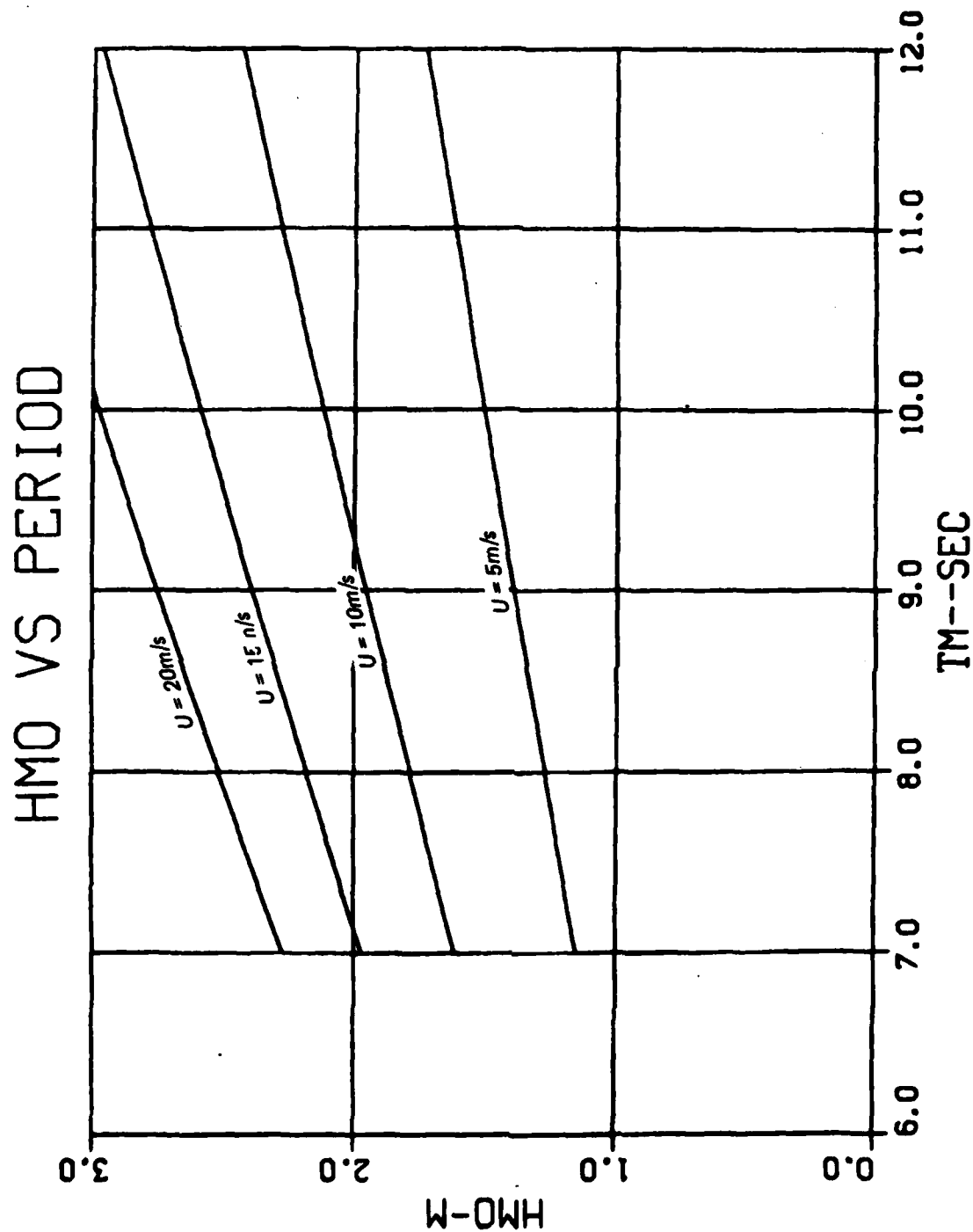


Figure 12. H_{mo} versus T_m as a function of windspeed
(depth = 5 m) (see Example 1)

The values for $H_{10\%}$ and $H_{1\%}$ are now found using the expressions given in the SPM (1984).

$$H_{10\%} = 1.27 H_s = 1.27(2.48) = 3.15 \text{ m (round off to 3.2 m) (10.3 ft)}$$

$$H_{1\%} = 1.67 H_s = 1.67(2.48) = 4.14 \text{ m (round off to 4.2 m) (13.6 ft)}$$

Note that the above calculations imply that the Rayleigh distribution of wave heights is valid under the given conditions, while the highest possible wave at this depth by monochromatic theory is about $0.76 (5 \text{ m}) = 3.8 \text{ m}$. Thus the tail of the wave height distribution will be truncated by breaking.

Design Example 3

Given

59. Determine the conditions under which a project built in 7 m (23 ft) of water would be subjected to breaking wave conditions (i.e., surf zone conditions) caused by irregular waves with a peak period of 11 sec.

Solution

60. The H_{mo} for the breaking limit (universal saturation) is found from Equation 38 as

$$H_{mo} = Bh = 0.6 (7 \text{ m}) = 4.2 \text{ m (13.8 ft)}$$

The spectral parameter α can be found from Equation 41 with ω_{hm} determined from Equation 42, i.e.,

$$\omega_{hm} = 2\pi f_m \left(\frac{h}{g} \right)^{1/2} = \frac{2\pi}{11} \left(\frac{7}{9.81} \right)^{1/2} = 0.4825$$

$$\alpha = \left(B\omega_{hm}/2 \right)^2 = \left[(0.6)(0.4825)/2 \right]^2 = 0.021$$

61. Next, use Equation 22 to find what value of κ will produce the following value of α at the given depth and peak period:

$$\alpha = 0.0078\kappa^{0.49}$$

or

$$\kappa = (\alpha/0.0078)^{1/0.49} = (0.021/0.0078)^{1/0.49} = 7.55$$

From Equation 24 with

$$k_m = \frac{2\pi}{L_m} = \frac{2\pi}{(gh)^{1/2} T_m} = \frac{2\pi}{[(9.81)(7)]^{1/2} (11)} = 0.0689 \text{ rad/m}$$

we get

$$U = (\kappa g/k_m)^{1/2} = [(7.55)(9.81)/0.689]^{1/2} = 32.8 \text{ m/sec (107.6 ft/sec)}$$

This windspeed is the sustained wind necessary to develop the equilibrium breaking condition at the site for the given peak period. It corresponds to speeds on the order of 73 mph which is a full hurricane force wind.

Design Example 4

Given

62. A wind sea has a significant wave height H_{mo} of 2 m and a peak spectral period T_m of 8 sec in a water depth of 10 m. Determine the corresponding H_{mo} in 4-m water depth, assuming no refraction or diffraction and that the peak period remains constant.

Solution

63. From Equation 29,

$$H_1 = \frac{1}{\pi} (\alpha_1)^{1/2} L_1 \quad \text{and} \quad H_2 = \frac{1}{\pi} (\alpha_2)^{1/2} L_2$$

Let

in 10 m

$$H_1 = H_{mo}$$

$$\alpha_1 = \alpha$$

$$L_1 = L_m$$

in 4 m

$$H_2 = H_{mo}$$

$$\alpha_2 = \alpha$$

$$L_2 = L_m$$

Taking the ratio of these two relationships yields

$$\frac{H_1}{H_2} = \left(\frac{\alpha_1}{\alpha_2} \right)^{1/2} \left(\frac{L_1}{L_2} \right)$$

64. The ratio α_1/α_2 can be found using Equation 22 as

$$\frac{\alpha_1}{\alpha_2} = \left(\frac{L_2}{L_1} \right)^{1/2}$$

Substituting this relationship into the previous equation gives

$$\frac{H_1}{H_2} = \left(\frac{L_1}{L_2} \right)^{3/4}$$

which is good under the restrictive assumptions of no refraction and diffraction and that the wind is equal and constant at both sites.

65. Using linear wave theory to find the wavelength associated with the peak spectral period (assumed to remain constant at 8 sec):

$$L_1 = 70.9 \text{ m at } h = 10 \text{ m}$$

$$L_2 = 48.0 \text{ m at } h = 4 \text{ m}$$

Thus

$$\frac{H_1}{H_2} = \left(\frac{70.9}{48.0} \right)^{3/4} = 1.34$$

so that

$$H_2 = \frac{H_1}{1.34} = \frac{2 \text{ m}}{1.34} = 1.5 \text{ m} \approx H_{mo} \text{ at a water depth } h = 4 \text{ m}$$

If the significant wave height had been shoaled using linear wave theory, H_1/H_2 would have been 0.7 and H_{mo} at $h = 4 \text{ m}$ would have been 2.9 m.

PART VI: SUMMARY

66. Recent work by Bouws et al. has led to a self-similar equilibrium spectral form for all water depths. This form, called the TMA spectrum, arises from the substitution of Kitaigorodskii et al.'s finite depth equilibrium range for the deepwater equilibrium range in the JONSWAP energy density equation. Examination of over 2,800 field spectra in varying water depths and under diverse conditions resulted in a parameterization for the spectral variables in terms of depth, peak frequency, and windspeed. The parameters α and γ were also expressed in terms of significant wave steepness. A simple expression for the energy-based significant wave height H_{mo} was derived from the TMA spectral form making it possible to predict the depth-limited equilibrium H_{mo} in either intermediate or shallow water.

67. The TMA spectral representation recovers the deepwater fully developed results when the deepwater limits are applied, and it follows the fully developed shallow-water empirical results when the suggested cutoff frequency relationship for shallow water is applied.

68. Within the surf zone the TMA spectrum can be fit rather well up to twice the peak frequency. Beyond that point highly nonlinear processes cause a deviation from the TMA form. A distinction was made between local and universal saturation, and a method of estimating the spectral parameters within the surf zone was presented.

69. The success of the TMA spectrum as a simple spectral model reinforces Kitaigorodskii et al.'s (1975) conclusion that the basic self-similarity scaling is in k -space. Many of the principal physical processes which bring about the TMA form have been identified but not quantified. Applications and examples were presented to illustrate some uses of the TMA results under the stated assumptions and limitations.

REFERENCES

- Bouws, E., et al. 1985a. "Similarity of the Wind Wave Spectrum in Finite Depth Water, Part I - Spectral Form," Journal of Geophysical Research, Vol 90, No. C1, pp 975-986.
- Bouws, E., et al. 1985b (in review). "Similarity of the Wind Wave Spectrum in Finite Depth Water, Part II - Quasi-Equilibrium Relations," Journal of Geophysical Research.
- Bretschneider, C. L. 1958. "Revisions in Wave Forecasting: Deep and Shallow Water," Proceedings of the 6th Conference on Coastal Engineering, American Society of Civil Engineers, pp 30-67.
- Gadzhiyev, Y. Z., and Kratsitsky, B. B. 1978. "The Equilibrium Range of the Frequency Spectra of Wind-Generated Waves in a Sea of Finite Depth," Izvestiya, Atmospheric and Ocean Physics, USSR, Vol 14, No. 3, pp 238-242.
- Hasselmann, K., et al. 1973. "Measurements of Wind Wave Growth and Swell Decay During the Joint Sea Wave Project (JONSWAP)," Report No. 12, Deutsches Hydrographisches Institut, Hamburg.
- Huang, N. E., et al. 1981. "A Unified Two-Parameter Wave Spectral Model for a General Sea State," Journal of Fluid Mechanics, Vol 112, pp 203-224.
- Kitaigorodskii, S. A., Krasitskii, V. P., and Zaslavskii, M. M. 1975. "On Phillip's Theory of Equilibrium Range in the Spectra of Wind-Generated Gravity Waves," Journal of Physical Oceanography, Vol 5, pp 410-420.
- Kruseman, P. 1976. "Two Practical Methods of Forecasting Wave Components with Periods Between 10 and 25 Seconds Near Hoek van Holland," Wetenschappelijk Rapport 76-1, Koninklijk Nederlands Meteorologisch Instituut, The Netherlands.
- Louguet-Higgins, M. S. 1952. "On the Statistical Distribution of the Heights of Sea Waves," Journal of Marine Research, Vol XI, No. 3, pp 245-266.
- Mitsuyasu, H. 1981. "Directional Spectra of Ocean Waves in Generation Area," Proceedings of the Conference on Directional Wave Spectra Applications, American Society of Civil Engineers, pp 87-101.
- Phillips, O. M. 1958. "The Equilibrium Range in the Spectrum of Wind-Generated Ocean Waves," Journal of Fluid Mechanics, Vol 4, pp 426-434.
- Pierson, W. J. and Moskowitz, L. 1964. "A Proposed Spectral Form for Fully Developed Windseas Based on the Similarity Theory of S. A. Kitaigorodskii," Journal of Geophysical Research, Vol 69, pp 5181-5190.
- Shore Protection Manual. 1984. 4th ed., 2 vols, US Army Engineer Waterways Experiment Station, Coastal Engineering Research Center, US Government Printing Office, Washington, DC.
- Thompson, E. F. 1980. "Energy Spectra in Shallow US Coastal Waters," Technical Paper 80-2, US Army Engineer Waterways Experiment Station, Coastal Engineering Research Center, Vicksburg, Miss.
- Thompson, E. F. and Vincent, C. L. 1983. "Prediction of Wave Height in Shallow Water," Proceedings of Coastal Structures '83, American Society of Civil Engineers, pp 1000-1008.

- Thompson, E. F. and Vincent, C. L. 1985. "Significant Wave Height for Shallow Water Design," Journal of the Waterway, Port, Coastal, and Ocean Division, American Society of Civil Engineers, Vol III, No. 5.
- Thornton, E. B. and Guza, R. T. 1982. "Energy Saturation and Phase Speeds Measured on a Natural Beach," Journal of Geophysical Research, Vol 87, No. C12, pp 9499-9508.
- Toba, Y. 1973. "Local Balance in the Air-Sea Boundary Processes: III - On the Spectrum of Wind Waves," Journal of the Oceanographic Society of Japan, Vol 29, pp 209-220.
- Vincent, C. L. 1982. "Depth-Limited Significant Wave Height: A Spectral Approach," Technical Report 82-3, US Army Engineer Waterways Experiment Station, Coastal Engineering Research Center, Vicksburg, Miss.
- _____. 1984. "Shoaling and Transmission of Wind Seas," 3rd Conference on Meteorology of the Coastal Zone, American Meteorological Society, pp 41-43, Miami, Fla.
- _____. 1985a. "Equilibrium Range Coefficient of Wind Wave Spectra in Water of Finite Depth," submitted to Journal of Geophysical Research.
- _____. 1985b (accepted for publication). "Energy Saturation of Irregular Waves During Shoaling," American Society of Civil Engineers.
- Vincent, C. L., and Hughes, S. A. 1985. "A Note on Wind Wave Growth in Shallow Water," Journal of Waterway, Port, Coastal and Ocean Division, American Society of Civil Engineers, Vol III, No. 4.
- Vincent, C. L. and Lockhart, J. H. 1984. "Determining Sheltered Water Wave Characteristics," ETL 1110-2-305, Headquarters, Department of the Army, Office Chief of Engineers, Washington, DC.

APPENDIX A: NOTATION

B	Parameter
\bar{d}	Relative depth
E	Total spectral energy
$E_J(f)$	Energy density for JONSWAP spectrum
$E_m(f)$	Equilibrium energy density in frequency space
$E_m(f,h)$	Finite depth equilibrium energy density in frequency space
$E_{pm}(f)$	Energy density for Pierson-Moskowitz spectrum
$E_{TMA}(f,h)$	Energy density for TMA spectrum
f	Frequency
f'	Frequency
F*	Highest frequency where shallow-water dispersion relation holds
f_c	Cut off frequency
F(k)	Equilibrium energy density in wave number space
f_m	Spectral peak frequency
g	Gravitational constant
h	Water depth
H_ℓ	H_{mo} for fully developed wind sea over a flat bottom
H_{max}	Maximum monochromatic wave height
H_{mo}	Zero-moment wave height
H_s	Average height of the 1/3 highest waves
$H_{1\%}$	Average of highest 1 percent of waves
$H_{10\%}$	Average of highest 10 percent of waves
k	Wave number
k_m	Wave number for waves at peak frequency
L	Wavelength
L_m	Wavelength associated with frequency f_m by linear wave theory
L_{mo}	Deepwater equivalent of L_m
R_{max}	Relative maximum wave height for monochromatic waves
R_{ms}	Ratio of H_{max} to H_s
R_{so}	Ratio of H_s to H_{mo}
T'	Period
T_m	Spectral peak period
U	10-m-high windspeed
X	Fetch distance
α	Spectral parameter
β	A constant

γ	Spectral parameter
ϵ	Significant wave steepness
κ	Dimensionless wave number
π	3.14...
σ	Spectral parameter
σ_a	Spectral parameter
σ_b	Spectral parameter
$\phi(2\pi f, h)$	Finite depth factor
ω	Circular frequency
ω_h	Depth dependent frequency
ω_{hm}	ω_h evaluated at f_m